



DYNAMIC RESPONSE OF REISSNER–MINDLIN PLATES UNDER THERMOMECHANICAL LOADING AND RESTING ON ELASTIC FOUNDATIONS

HUI-SHEN SHEN, J. YANG AND L. ZHANG

School of Civil Engineering and Mechanics, Shanghai Jiao Tong University, Shanghai 200030, People's Republic of China

(Received 9 June 1999, and in final form 30 August 1999)

This paper deals with the dynamic response of Reissner–Mindlin plates exposed to thermomechanical loading and resting on a Pasternak-type elastic foundation. The mechanical loads consist of transverse partially distributed impulsive loads and in-plane edge loads while the temperature field is assumed to exhibit a linear variation through the thickness of the plate. The formulations are based on the Reissner–Mindlin plate theory, considering the first order shear deformation effect and including the plate–foundation interaction and thermal effects. The Modal Superposition Approach and State Variable Approach are both used to determine the dynamic response of the plate. Some subset problems such as buckling, free vibration and static bending are also discussed and the solutions are given in closed form. The numerical illustrations concern moderately thick plates with all four edges simply supported and resting on Pasternak-type elastic foundations with the Winkler elastic foundations being a limiting case. Effects of foundation stiffness, transverse shear deformation, plate aspect ratio, shape and duration of impulsive load, loaded area, and initial membrane stress as well as thermal bending stress on the dynamic response of Reissner–Mindlin plates are studied.

© 2000 Academic Press

1. INTRODUCTION

Moderately thick plates are widely used in civil engineering. A typical plate structure is the concrete pavement of an airfield. During their operational life, these plates are subjected to external pressure, especially impulsive loads (such as landings of airplane), temperature field (such as sunshine) and in-plane edge loads. The problem is usually simplified and analyzed as a thick rectangular plate supported by an elastic foundation. For this reason, the study of the dynamic response of moderately thick plates under complex loading conditions and resting on an elastic foundation is a matter of considerable importance in the design of concrete pavements of airfields.

Many publications have appeared in the literature on the dynamic response of isotropic and composite laminated thick plates, e.g., Dobyns [1]. However, investigations of dynamic response of initially stressed thick plates are very limited and most of these works are under the loading condition of in-plane edge loads combined with transverse forces. Reismann and Tendorf [2] gave the solution of the force motion problem of isotropic thick plates under initial membrane stress using a Modal Superposition Approach (MSA). As pointed out by Chen and Dawe [3], MSA relies on a transformation of the coupled set of structure dynamic equation, written in terms of physical displacements, into an uncoupled set of equations, written in terms of generalized displacements. Sun and Whitney [4] used MSA to study the effects of initial tensile stress on the dynamic response of an infinitely long,

simply supported composite plate under cylindrical bending. Khdeir and Reddy [5] studied the transient response of simply supported antisymmetric angle-ply laminated plates with or without in-plane edge loads using a State Variable Approach (SVA). It has been shown that MSA and SVA are efficient techniques for dynamic analysis of the plate, but all the above-mentioned investigations concern the plate without elastic foundations and none of them include the thermal effects. Xiang *et al.* [6] gave solutions for the vibration problem of initially compressive stressed isotropic thick plates resting on Pasternak-type elastic foundations. Librescu and Lin [7] and Librescu *et al.* [8], respectively, studied the non-linear vibration behavior of flat and curved panels with or without elastic foundation and subjected to thermomechanical loading.

This paper deals with the dynamic response of Reissner–Mindlin plates exposed to thermomechanical loading and resting on a Pasternak-type elastic foundation. The mechanical loads consist of transverse partially distributed impulsive loads and in-plane edge loads while the temperature field is assumed to exhibit a linear variation through the thickness of the plate. The material properties are assumed to be independent of temperature. The formulations are based on Reissner–Mindlin first order shear deformation plate theory (FSDPT) and include the plate–foundation interaction and thermal effects. The MSA and SVA are extended to the case of Reissner–Mindlin plates subjected to complex loading and resting on a Pasternak-type elastic foundation. Some subset problems such as buckling, free vibration and static bending are discussed, and the solutions are given in closed form. Numerical examples are presented that relate to the dynamic behaviours of simply supported moderately thick plates resting on Pasternak-type elastic foundations from which results for Winkler foundations are obtained as a limiting case.

2. ANALYTICAL FORMULATION

2.1. GOVERNING EQUATIONS

Consider a moderately thick rectangular plate of length a , width b , and thickness h , simply supported at four edges and resting on a Pasternak-type elastic foundation. The plate is exposed to a stationary temperature field $T(X, Y, Z)$ and impulsive load q over a central area $a_1 \times b_1$, as shown in Figure 1, combined with in-plane edge loads N_x in the

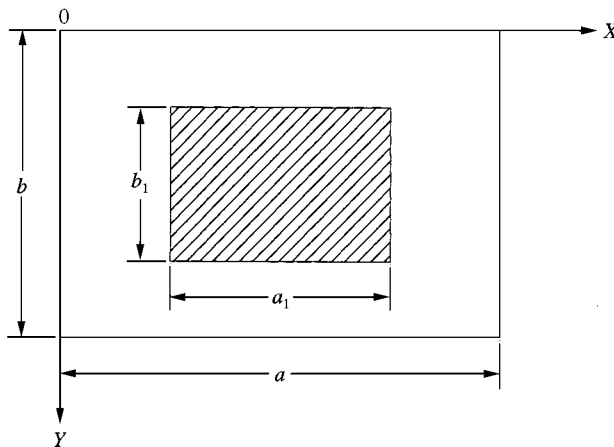


Figure 1. A Reissner–Mindlin plate subjected to a transverse partially distributed impulsive load.

X direction and N_Y in the Y direction. As is customary [6, 7, 9–11], the foundation is assumed to be attached to the plate and separation does not arise. The load–displacement relationship of the foundation is assumed to be $p = \bar{K}_1 \bar{W} - \bar{K}_2 \nabla^2 \bar{W}$, where \bar{W} is the plate deflection, p is the force per unit area, \bar{K}_1 is the Winkler foundation stiffness, \bar{K}_2 is a constant showing the effect of the shear interactions of the vertical elements, ∇^2 is the Laplace operator in X and Y , $\bar{\Psi}_X$ and $\bar{\Psi}_Y$ are the mid-plane rotations of the normals about the \bar{Y} and \bar{X} axis respectively. \bar{t} is the time and Ω is the frequency.

It is postulated that the temperature field $T(X, Y, Z)$ exhibits a linear variation through the plate thickness, i.e.,

$$T(X, Y, Z) = T_0 \left(1 + C \frac{Z}{h} \right), \tag{1}$$

in which T_0 and C denote the temperature amplitude and gradient respectively.

The thermal moments caused by the temperature field $T(X, Y, Z)$ are defined by

$$\bar{M}^T = \frac{E\alpha}{1-\nu} \int_{-h/2}^{h/2} ZT(X, Y, Z) dZ, \tag{2}$$

where α is the thermal expansion coefficient of a plate, E is Young’s modulus and ν is the Poisson’s ratio.

The deduction of the governing equations associated with Reissner–Mindlin first order shear deformation plate theory, and including the plate–foundation interaction and thermal effects, follows the same pattern in the case of its static counterpart [11], so that the motion equations can be written as

$$L_{11}(\bar{\Psi}_X) + L_{12}(\bar{\Psi}_Y) + L_{13}(\bar{W}) - \bar{K}_1 \bar{W} + \bar{K}_2 \nabla^2 \bar{W} + q = L_{14}(\bar{W}), \tag{3}$$

$$L_{21}(\bar{\Psi}_X) + L_{22}(\bar{\Psi}_Y) + L_{23}(\bar{W}) - \bar{M}_{,X}^T = L_{24}(\bar{\Psi}_X), \tag{4}$$

$$L_{31}(\bar{\Psi}_X) + L_{32}(\bar{\Psi}_Y) + L_{33}(\bar{W}) - \bar{M}_{,Y}^T = L_{34}(\bar{\Psi}_Y), \tag{5}$$

where

$$\begin{aligned} L_{11}(\) &= \kappa^2 Gh \frac{\partial}{\partial X}, & L_{12}(\) &= \kappa^2 Gh \frac{\partial}{\partial Y}, \\ L_{13}(\) &= (\kappa^2 Gh + N_X) \frac{\partial^2}{\partial X^2} + (\kappa^2 Gh + N_Y) \frac{\partial^2}{\partial Y^2}, & L_{14}(\) &= I_1 \frac{\partial^2}{\partial \bar{t}^2}, \\ L_{21}(\) &= D \left(\frac{\partial^2}{\partial X^2} + \frac{1-\nu}{2} \frac{\partial^2}{\partial Y^2} \right) - \kappa^2 Gh, & L_{23}(\) &= -\kappa^2 Gh \frac{\partial}{\partial X}, \\ L_{31}(\) &= L_{22}(\) = \frac{1+\nu}{2} D \frac{\partial}{\partial X \partial Y}, & L_{32}(\) &= D \left(\frac{1-\nu}{2} \frac{\partial^2}{\partial X^2} + \frac{\partial^2}{\partial Y^2} \right) - \kappa^2 Gh, \\ L_{33}(\) &= -\kappa^2 Gh \frac{\partial}{\partial Y}, & L_{34}(\) = L_{24}(\) &= I_3 \frac{\partial^2}{\partial \bar{t}^2}, & \nabla^2 &= \frac{\partial^2}{\partial X^2} + \frac{\partial^2}{\partial Y^2}, \end{aligned} \tag{6}$$

in which

$$D = \frac{Eh^3}{12(1-\nu^2)}, \quad (I_1, I_3) = \int_{-h/2}^{h/2} \rho(1, Z^2) dZ, \quad (7)$$

D is flexural rigidity, G is shear modulus, and ρ is the mass density of the plate. Also, κ^2 is the shear factor, which accounts for the non-uniformity of the shear strain distribution through the plate thickness. For Reissner plate theory $\kappa^2 = \frac{5}{6}$ while for Mindlin plate theory $\kappa^2 = \pi^2/12$.

The stress resultants are

$$\bar{M}_X = D \left(\frac{\partial \bar{\Psi}_X}{\partial X} + \nu \frac{\partial \bar{\Psi}_Y}{\partial Y} \right) - \bar{M}^T, \quad (8)$$

$$\bar{M}_Y = D \left(\nu \frac{\partial \bar{\Psi}_X}{\partial X} + \frac{\partial \bar{\Psi}_Y}{\partial Y} \right) - \bar{M}^T, \quad (9)$$

$$\bar{M}_{XY} = \frac{(1-\nu)}{2} D \left(\frac{\partial \bar{\Psi}_X}{\partial Y} + \frac{\partial \bar{\Psi}_Y}{\partial X} \right), \quad (10)$$

$$\bar{Q}_X = \kappa^2 Gh \left(\frac{\partial \bar{W}}{\partial X} + \bar{\Psi}_X \right), \quad (11)$$

$$\bar{Q}_Y = \kappa^2 Gh \left(\frac{\partial \bar{W}}{\partial Y} + \bar{\Psi}_Y \right). \quad (12)$$

If all four edges of the plate are simply supported and “movable”, the boundary conditions are

$X = 0, a$:

$$\bar{W} = 0, \quad \bar{\Psi}_Y = 0, \quad \bar{M}_X = 0, \quad (13a)$$

$Y = 0, b$:

$$\bar{W} = 0, \quad \bar{\Psi}_X = 0, \quad \bar{M}_Y = 0. \quad (13b)$$

Introducing dimensionless quantities (in which the alternative forms k_1 and k_2 are not needed until the numerical examples are considered),

$$x = \pi \frac{X}{a}, \quad y = \pi \frac{Y}{b}, \quad \beta = \frac{a}{b}, \quad \theta = \frac{\sqrt{12}a}{\pi h}, \quad y = \frac{\pi^2 D}{a^2 \kappa^2 Gh}, \quad (\nu_1, \nu_2) = \left(\frac{1-\nu}{2}, \frac{1+\nu}{2} \right),$$

$$W = \frac{\bar{W}}{h}, \quad (\Psi_x, \Psi_y) = (\bar{\Psi}_X, \bar{\Psi}_Y) \frac{a}{\pi h}, \quad (Q_x, Q_y) = (\bar{Q}_X, \bar{Q}_Y) \frac{a}{\pi \kappa^2 Gh^2},$$

$$(M_x, M_y, M_{xy}, M^T) = (\bar{M}_X, \bar{M}_Y, \bar{M}_{XY}, \bar{M}^T) \frac{a^2}{\pi^2 Dh}, \quad (K_1, k_1) = (a^4, b^4) \frac{\bar{K}_1}{\pi^4 D},$$

$$(K_2, k_2) = (a^2, b^2) \frac{\bar{K}_2}{\pi^2 D}, \quad t = \frac{\bar{t}\pi}{a} \sqrt{\frac{E}{\rho(1-\nu^2)}}, \quad \omega^2 = \Omega^2 \frac{\rho a^2(1-\nu^2)}{\pi^2 E},$$

$$\lambda_q = \frac{qa^4}{\pi^4 Dh}, \quad \lambda_x = \frac{N_x a^2}{\pi^2 D}, \quad \lambda_y = \frac{N_y b^2}{\pi^2 D} \quad (14)$$

enables equations (3)–(5) to be written in dimensionless forms as

$$L_{11}(\Psi_x) + L_{12}(\Psi_y) + L_{13}(W) - K_1 W + K_2 \bar{V}^2 W + \lambda_q = L_{14}(W), \quad (15)$$

$$L_{21}(\Psi_x) + L_{22}(\Psi_y) + L_{23}(W) - M_{,x}^T = L_{24}(\Psi_x), \quad (16)$$

$$L_{31}(\Psi_x) + L_{32}(\Psi_y) + L_{33}(W) - M_{,y}^T = L_{34}(\Psi_y), \quad (17)$$

where

$$L_{11}(\cdot) = \frac{1}{\gamma} \frac{\partial}{\partial x}, \quad L_{12}(\cdot) = \frac{\beta}{\gamma} \frac{\partial}{\partial y}, \quad L_{13}(\cdot) = \left(\frac{1}{\gamma} + \lambda_x \right) \frac{\partial^2}{\partial x^2} + \left(\frac{1}{\gamma} + \lambda_y \beta^2 \right) \beta^2 \frac{\partial^2}{\partial y^2},$$

$$L_{14}(\cdot) = \theta^2 \frac{\partial^2}{\partial t^2}, \quad L_{21}(\cdot) = \left(\frac{\partial^2}{\partial x^2} + \nu_1 \beta^2 \frac{\partial^2}{\partial y^2} \right) - \frac{1}{\gamma}, \quad L_{23}(\cdot) = -\frac{1}{\gamma} \frac{\partial}{\partial x},$$

$$L_{31}(\cdot) = L_{22}(\cdot) = \nu_2 \beta \frac{\partial}{\partial x \partial y}, \quad L_{32}(\cdot) = \left(\nu_1 \frac{\partial^2}{\partial x^2} + \beta^2 \frac{\partial^2}{\partial y^2} \right) - \frac{1}{\gamma}, \quad L_{33}(\cdot) = -\frac{\beta}{\gamma} \frac{\partial}{\partial y},$$

$$L_{34}(\cdot) = L_{24}(\cdot) = \frac{\partial^2}{\partial t^2}, \quad \bar{V}^2 = \frac{\partial^2}{\partial x^2} + \beta^2 \frac{\partial^2}{\partial y^2} \quad (18)$$

and the dimensionless forms of stress resultants become

$$M_x = \frac{\partial \Psi_x}{\partial x} + \nu \beta \frac{\partial \Psi_y}{\partial y} - M^T, \quad (19)$$

$$M_y = \nu \frac{\partial \Psi_x}{\partial x} + \beta \frac{\partial \Psi_y}{\partial y} - M^T, \quad (20)$$

$$M_{xy} = \nu_1 \left(\beta \frac{\partial \Psi_x}{\partial y} + \frac{\partial \Psi_y}{\partial x} \right), \quad (21)$$

$$Q_x = \frac{\partial W}{\partial x} + \Psi_x, \quad (22)$$

$$Q_y = \beta \frac{\partial W}{\partial y} + \Psi_y. \quad (23)$$

The boundary conditions of equation (13) become

$x = 0, \pi$:

$$W = 0, \quad \Psi_y = 0, \quad M_x = 0, \tag{24a}$$

$y = 0, \pi$:

$$W = 0, \quad \Psi_x = 0, \quad M_y = 0, \tag{24b}$$

We expand the constant thermal bending moment in the double Fourier sine series as

$$M^T(x, y) = \sum_{i=1,3,\dots}^{\infty} \sum_{j=1,3,\dots}^{\infty} c_{ij} \sin ix \sin jy, \tag{25}$$

where

$$c_{ij} = \frac{16M^T}{\pi^2 ij} \quad (i, j = \text{odd}). \tag{26}$$

Substituting equation (25) into equation (24), the homogeneous forms of boundary conditions can be obtained.

2.2. MODAL SUPERPOSITION APPROACH (MSA)

It is assumed that the solutions of equation (15)–(17) have the forms [2–4]

$$W(x, y, t) = \sum_{m=1}^{\infty} \sum_{n=1}^{\infty} \sum_{p=1}^3 W_{mn}^{(p)}(x, y) T_{mn}^{(p)}(t), \tag{27a}$$

$$\Psi_x(x, y, t) = \sum_{m=1}^{\infty} \sum_{n=1}^{\infty} \sum_{p=1}^3 \Psi_{xmn}^{(p)}(x, y) T_{mn}^{(p)}(t), \tag{27b}$$

$$\Psi_y(x, y, t) = \sum_{m=1}^{\infty} \sum_{n=1}^{\infty} \sum_{p=1}^3 \Psi_{ymn}^{(p)}(x, y) T_{mn}^{(p)}(t), \tag{27c}$$

where $W_{mn}^{(p)}(x, y)$, $\Psi_{xmn}^{(p)}(x, y)$, $\Psi_{ymn}^{(p)}(x, y)$ are the p th order shape functions and $T_{mn}^{(p)}(t)$ is the p th order principal co-ordinate for the (m, n) modal, and $\omega_{mn}^{(p)}$ is the frequency of the plate.

Substituting equation (27) into equations (15)–(17) yields

$$\sum_{m=1}^{\infty} \sum_{n=1}^{\infty} \sum_{p=1}^3 [\ddot{T}_{mn}^{(p)}(t) + (\omega_{mn}^{(p)})^2 T_{mn}^{(p)}(t)] \theta^2 W_{mn}^{(p)}(x, y) - \lambda_q = 0, \tag{28}$$

$$\sum_{m=1}^{\infty} \sum_{n=1}^{\infty} \sum_{p=1}^3 [\ddot{T}_{mn}^{(p)}(t) + (\omega_{mn}^{(p)})^2 T_{mn}^{(p)}(t)] \Psi_{xmn}^{(p)}(x, y) + \frac{16M^T}{\pi^2} \sum_{i=1,3}^{\infty} \sum_{j=1,3}^{\infty} \frac{\cos ix \sin jy}{j} = 0, \tag{29}$$

$$\sum_{m=1}^{\infty} \sum_{n=1}^{\infty} \sum_{p=1}^3 [\ddot{T}_{mn}^{(p)}(t) + (\omega_{mn}^{(p)})^2 T_{mn}^{(p)}(t)] \Psi_{ymn}^{(p)}(x, y) + \frac{16\beta M^T}{\pi^2} \sum_{i=1,3}^{\infty} \sum_{j=1,3}^{\infty} \frac{\cos ix \sin jy}{i} = 0, \tag{30}$$

in which a superposed dot indicates differentiation with respect to time. It is noted that, because of equations (A3) and (A4), $W_{mn}^{(p)}(x, y)$, $\Psi_{xmn}^{(p)}(x, y)$ and $\Psi_{ymn}^{(p)}(x, y)$ are dependent on foundation stiffness K_1 and K_2 .

Multiplying equation (28) by $W_{kl}^{(q)}(x, y)$, equation (29) by $\Psi_{xkl}^{(q)}(x, y)$, and equation (30) by $\Psi_{jkl}^{(q)}(x, y)$, respectively, and then adding all these three equations and integrating over the plate area, we may drop the summation by the orthogonality condition (see Appendix A), and obtain

$$\ddot{T}_{mn}^{(p)}(t) + (\omega_{mn}^{(p)})^2 T_{mn}^{(p)}(t) = \frac{Q_{mn}^{(p)}}{K_{mn}^{(p)}}, \tag{31}$$

where

$$Q_{mn}^{(p)} = \int_0^\pi \int_0^\pi \left\{ \lambda_q(x, y, t) W_{mn}^{(p)}(x, y) - \frac{16M^T}{\pi^2} \left[\Psi_{xmn}^{(p)}(x, y) \sum_{i=1,3}^\infty \sum_{j=1,3}^\infty \frac{\cos ix \sin jy}{j} + \beta \Psi_{ymn}^{(p)}(x, y) \sum_{i=1,3}^\infty \sum_{j=1,3}^\infty \frac{\sin ix \cos jy}{i} \right] \right\} dx dy, \tag{32a}$$

$$K_{mn}^{(p)} = \int_0^\pi \int_0^\pi [\theta^2 (W_{mn}^{(p)}(x, y))^2 + (\Psi_{xmn}^{(p)}(x, y))^2 + (\Psi_{ymn}^{(p)}(x, y))^2] dx dy. \tag{32b}$$

Zero initial conditions are assumed, i.e.,

$$(W, \Psi_x, \Psi_y)|_{t=0} = 0. \quad \left(\frac{\partial W}{\partial t}, \frac{\partial \Psi_x}{\partial t}, \frac{\partial \Psi_y}{\partial t} \right) \Big|_{t=0} = 0 \tag{33a,b}$$

from equation (31), we can obtain

$$T_{mn}^{(p)} = \frac{1}{\omega_{mn}^{(p)} K_{mn}^{(p)}} \int_0^t Q_{mn}^{(p)}(\tau) \sin[\omega_{mn}^{(p)}(t - \tau)] d\tau. \tag{34}$$

Substituting equation (34) into equation (27), $W(x, y, t)$, $\Psi_x(x, y, t)$ and $\Psi_y(x, y, t)$ can be obtained.

2.3. STATE VARIABLE APPROACH (SVA)

Following Khdeir and Reddy [5, 16, 17] the solutions of equations (15)–(17) are assumed to have the forms

$$\begin{aligned} W(x, y, t) &= \sum_{m,n=1}^\infty W_{mn}(t) \sin mx \sin ny, \\ \Psi_x(x, y, t) &= \sum_{m,n=1}^\infty \Psi_{x_{mn}}(t) \cos mx \sin ny, \\ \Psi_y(x, y, t) &= \sum_{m,n=1}^\infty \Psi_{y_{mn}}(t) \sin mx \cos ny, \end{aligned} \tag{35}$$

$$\lambda_q(x, y, t) = \sum_{m,n=1}^{\infty} \lambda_{qmn}(t) \sin mx \sin ny,$$

$$M^T(x, y, t) = \sum_{m,n=1}^{\infty} M_{mn}^T(t) \sin mx \sin ny,$$

where $W_{mn}(t)$, $\Psi_{xmn}(t)$ and $\Psi_{ymn}(t)$ are unknown functions, and $\lambda_{qmn}(t)$ and $M_{mn}^T(t)$ are the coefficients of the Fourier expansion of λ_q and M^T . Substituting equation (35) into equations (15)–(17) yields

$$\ddot{W}_{mn}(t) = -a_{11}W_{mn}(t) - a_{12}\Psi_{xmn}(t) - a_{13}\Psi_{ymn}(t) + \frac{\lambda_{qmn}(t)}{\theta^2}, \tag{36}$$

$$\ddot{\Psi}_{xmn}(t) = -a_{21}W_{mn}(t) - a_{22}\Psi_{xmn}(t) - a_{23}\Psi_{ymn}(t) - mM_{mn}^T, \tag{37}$$

$$\ddot{\Psi}_{ymn}(t) = -a_{31}W_{mn}(t) - a_{32}\Psi_{xmn}(t) - a_{33}\Psi_{ymn}(t) - n\beta M_{mn}^T. \tag{38}$$

In equations (36)–(38) and (45) below, $a_{ij}(i, j = 1, 2, 3)$ is taken from equation (A4) in Appendix A. Let

$$\{Z_1(t), Z_2(t), Z_3(t), Z_4(t), Z_5(t), Z_6(t)\}^T = \{W_{mn}(x), \Psi_{xmn}(t), \Psi_{ymn}(t), \dot{W}_{mn}(x), \dot{\Psi}_{xmn}(t), \dot{\Psi}_{ymn}(t)\}^T \tag{39}$$

then equations (36)–(38) can be written as

$$\dot{\mathbf{Z}} = \mathbf{AZ} + \mathbf{b}, \tag{40}$$

where

$$\mathbf{Z} = \{Z_1(t), Z_2(t), Z_3(t), Z_4(t), Z_5(t), Z_6(t)\}^T, \tag{41a}$$

$$\mathbf{A} = \begin{bmatrix} 0 & 0 & 0 & 1 & 0 & 0 \\ 0 & 0 & 0 & 0 & 1 & 0 \\ 0 & 0 & 0 & 0 & 0 & 1 \\ -a_{11} & -a_{12} & -a_{13} & 0 & 0 & 0 \\ -a_{21} & -a_{22} & -a_{23} & 0 & 0 & 0 \\ -a_{31} & -a_{32} & -a_{33} & 0 & 0 & 0 \end{bmatrix}, \tag{41b}$$

$$\mathbf{b} = \left\{ 0, 0, 0, \frac{\lambda_{qmn}(t)}{\theta^2}, -mM_{mn}^T, -n\beta M_{mn}^T \right\}. \tag{41c}$$

Using the same procedure as in references [5, 16, 17], the solution of equation (35) can be obtained as

$$\mathbf{Z}(t) = \int_0^t e^{\mathbf{A}(t-\tau)} \mathbf{b}(\tau) d\tau. \tag{42}$$

2.4. SUBSET PROBLEMS

2.4.1. Buckling problem

If $q = 0$, $T_0 = 0$, and in-plane loads are compressive edge loads and $N_y = \chi N_x$, where χ is a constant (this means that the compressive loads in the X and Y directions vary proportionally), then the buckling load parameter can be written as

$$(\lambda_x)_{cr} = - \frac{(m^2 + n^2\beta^2)^2 + [K_1 + K_2(m^2 + n^2\beta^2)][1 + \gamma(m^2 + n^2\beta^2)]}{(m^2 + \chi n^2\beta^2)[1 + \gamma(m^2 + n^2\beta^2)]}. \tag{43}$$

Solution (43) is in accordance with that of Shen [9].

2.4.2. Free vibration problem

Neglecting the transverse impulsive loads and thermal loads, this problem degenerates to the vibration problem as previously reported in Xiang *et al.* [6]. The three frequencies can be explicitly calculated as

$$[\omega_{mn}]^2 = \begin{cases} \frac{1}{\gamma} + v_1(m^2 + n^2\beta^2), \\ b_1 \pm \sqrt{b_1^2 - b_2}, \end{cases} \tag{44a-c}$$

where

$$\begin{aligned} b_1 &= \frac{1}{2}(a_{11} + a_{22} + v_2 n^2\beta^2), \\ b_2 &= a_{11}(a_{22} + v_2 n^2\beta^2) - \theta^2(a_{12}^2 + a_{13}^2). \end{aligned} \tag{45a,b}$$

Solution (44) is in accordance with that of Xiang *et al.* [6].

2.4.3. Static bending problem

If q is a static pressure, then the bending problem of simply supported, moderately thick plates subjected to combined mechanical and thermal loads and resting on Pasternak-type foundations is now considered. The explicit form of solution is as follows:

$$\begin{aligned} W(x, y) &= \sum_{m,n=1}^{\infty} \frac{b_3(\gamma\lambda_{qmn} + M_{mn}^T) + \lambda_{qmn}}{\gamma b_5} \sin mx \sin ny, \\ \Psi_x(x, y) &= - \sum_{m,n=1}^{\infty} \frac{mM_{mn}^T[b_3(1 + \gamma K_2) + \gamma(b_4 + K_1)] + m\lambda_{qmn}}{\gamma b_5} \cos mx \sin ny, \\ \Psi_y(x, y) &= - \sum_{m,n=1}^{\infty} \frac{n\beta M_{mn}^T[b_3(1 + \gamma K_2) + \gamma(b_4 + K_1)] + n\beta\lambda_{qmn}}{\gamma b_5} \sin mx \cos ny, \end{aligned} \tag{46}$$

where

$$\begin{aligned}
 b_3 &= m^2 + n^2\beta^2, \\
 b_4 &= \lambda_x(m^2 + \chi n^2\beta^2)/\beta^2, \\
 b_5 &= b_3[b_3(1 + \gamma K_2) + \gamma b_4 + \gamma K_1 + K_2] + b_4 + K_1. \quad (47)
 \end{aligned}$$

3. NUMERICAL EXAMPLES AND COMMENTS

A dynamic analysis has been presented for a simply supported Reissner–Mindlin plate subjected to thermomechanical loading and resting on a Pasternak-type elastic foundation. A number of examples were solved to illustrate their application to the performance of moderately thick plates resting on Winkler or Pasternak-type elastic foundations. For all of the examples, $E = 3.5 \times 10^4 \text{ MN/m}^2$, $\nu = 0.15$, $\alpha = 1.0 \times 10^{-5} / ^\circ\text{C}$, $\rho = 2500 \text{ kg/m}^3$, and the transverse shear correction factor was considered to be $\kappa^2 = \pi^2/12$. The impulsive pressure $q(X, Y, \bar{t}) = q_0 F(\bar{t}) f(X, Y)$ is applied on the top surface of the plate, in which q_0 is the maximum amplitude $f(X, Y)$ is a unit function in space domain and $F(\bar{t})$ is a unit function in time domain which can be any one of the types listed in Table 1.

The convergence study of MSA and SVA used herein is demonstrated in Table 2. For this purpose, square plates with $b/h = 10$ subjected to a suddenly applied central patch load ($a_1/a = b_1/b = 0.5$) combined with in-plane uniaxial compression with or without initial thermal bending stress and resting on a Pasternak-type elastic foundation with $(k_1, k_2) = (2.0, 1.0)$, are considered. The results indicate that the convergence is attained by taking m and n up to 25 for the case of absence of initial thermal bending stress; in contrast, m and n will be taken up to 35 when initial thermal bending stress is present.

As part of the validation of the present method, the dimensionless central deflections and bending moments of a simply supported rectangular plate, subjected to a uniform step load over a central patch area alone and without an elastic foundation, are compared in Figure 2 with the three dimensional solutions of Reismann and Lee [18] and finite element results of Reddy [19], using their computing data $E = 1.0$, $\nu = 0.3$, $\rho = 1.0$, $a/b = \sqrt{2}$, $b/h = 5$. In Figure 2, the solutions of classical plate theory (CPT) are also shown. The dimensionless frequencies, deflections and bending moments of initially stressed, moderately thick rectangular plates subjected to a step load and without an elastic foundation are calculated and compared in Table 3 and Figure 3 with MSA solution of Reissmann and Tendorf [2] using their computing data, i.e., $\nu = 0.3$, $\kappa^2 = 0.86$, $a/h = 10$, $b/a = \sqrt{2}$, $a_1/a = 0.2$, $b_1/b = 0.141$. In addition, for the static thermal bending problem of foundationless plates, the central deflections, bending moments and shear forces at the edges are calculated and compared in Table 4 with the results given in Irschik and Pachinger [20]. The computing data are $b/a = 1.5$, $\nu = 0.3$, $h/a = 0.1$ and 0.3 , respectively. These three comparisons show that the present results agree well with the comparator solutions.

A parametric study intended to supply information on the dynamic behaviors of a moderately thick plate subjected to thermomechanical loading and resting on an elastic foundation was undertaken. The typical results are shown in Figures 4–12. It is mentioned that in all these figures $\bar{t}\sqrt{E/\rho}/b$, $\bar{W}Eah/q_0b^3$, $\bar{M}_x a^2/q_0b^2h^2$ represent the dimensionless forms of, respectively, time, central deflection and bending moment of the plate, i.e., at the point $(X, Y) = (a/2, b/2)$.

Figure 4 shows central deflection and bending moment as functions of time for an initially stressed thick square plate subjected to a suddenly applied central patch load and resting on

TABLE 1
The various kinds of pulse shapes of transverse impulsive loads

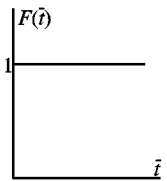
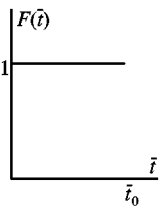
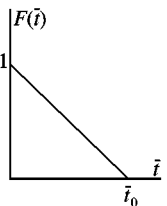
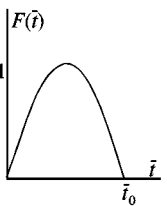
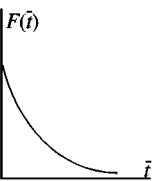
Case	1	2	3	4	5
	Sudden loads	Step loads	Triangular loads	Sine loads	Exponential loads
$F(\bar{t})$	 <p style="text-align: center;">$F(\bar{t}) = 1$</p>	 <p style="text-align: center;">$F(\bar{t}) = \begin{cases} 1, & \bar{t} \leq \bar{t}_0 \\ 0, & \bar{t} > \bar{t}_0 \end{cases}$</p>	 <p style="text-align: center;">$F(\bar{t}) = \begin{cases} 1 - \frac{\bar{t}}{\bar{t}_0}, & \bar{t} \leq \bar{t}_0 \\ 0, & \bar{t} > \bar{t}_0 \end{cases}$</p>	 <p style="text-align: center;">$F(\bar{t}) = \begin{cases} \sin \frac{\pi \bar{t}}{\bar{t}_0}, & \bar{t} \leq \bar{t}_0 \\ 0 & \bar{t} > \bar{t}_0 \end{cases}$</p>	 <p style="text-align: center;">$F(\bar{t}) = e^{-\alpha \bar{t}}$</p>

TABLE 2

Convergence study of center deflection and bending moment for a square moderately thick plate ($\beta = 1.0$, $b/h = 10.0$, $a_1/a = b_1/b = 0.5$, $N_X/(N_X)_{cr} = -0.25$, $T_0 = 30^\circ\text{C}$, $c = 5.0$, $(k_1, k_2) = (2.0, 1.0)$, $\tilde{W} = \bar{W}Eah/q_0b^3$, $\tilde{M}_X = \bar{M}_Xa^2/q_0b^2h^2$)

		$\bar{\tau}\sqrt{E/\rho}/b$	MSA					SVA					
			2	4	6	8	10	2	4	6	8	10	
m, n Up to 13	$c = 0$	\tilde{W}	1.4020	3.2821	2.5515	0.4442	0.4388	1.4020	3.2821	2.5515	0.4442	0.4388	
		\tilde{M}_X	1.4660	3.3783	2.6477	0.5390	0.4058	1.4659	3.3782	2.6473	0.5387	0.4061	
		$c = 5.0$	\tilde{W}	1.4709	3.4364	2.6598	0.4523	0.4549	1.4709	3.4364	2.6598	0.4523	0.4549
			\tilde{M}_X	1.3433	3.4221	2.4947	0.3739	0.2549	1.3433	3.4224	2.4947	0.3744	0.2553
m, n Up to 17	$c = 0$	\tilde{W}	1.4021	3.2820	2.5514	0.4441	0.4385	1.4021	3.2820	2.5514	0.4441	0.4385	
		\tilde{M}_X	1.4687	3.3802	2.6472	0.5372	0.3998	1.4691	3.3800	2.6474	0.5377	0.4003	
		$c = 5.0$	\tilde{W}	1.4710	3.4365	2.6597	0.4522	0.4543	1.4710	3.4365	2.6597	0.4521	0.4543
			\tilde{M}_X	1.3540	3.4218	2.4916	0.3714	0.2502	1.3539	3.4218	2.4918	0.3718	0.2516
m, n Up to 19	$c = 0$	\tilde{W}	1.4023	3.2821	2.5515	0.4442	0.4386	1.4023	3.2821	2.5515	0.4443	0.4386	
		\tilde{M}_X	1.4730	3.3803	2.6482	0.5401	0.4012	1.4734	3.3800	2.6482	0.5403	0.4014	
		$c = 5.0$	\tilde{W}	1.4711	3.4366	2.6598	0.4521	0.4543	1.4711	3.4366	2.6598	0.4521	0.4542
			\tilde{M}_X	1.3422	3.3963	2.4726	0.3601	0.2509	1.3421	3.3963	2.4727	0.3606	0.2511
m, n Up to 21	$c = 0$	\tilde{W}	1.4023	3.2821	2.5515	0.4442	0.4385	1.4023	3.2821	2.5515	0.4442	0.4385	
		\tilde{M}_X	1.4713	3.3784	2.6475	0.5384	0.4002	1.4715	3.3779	2.6479	0.5383	0.4004	
		$c = 5.0$	\tilde{W}	1.4711	3.4365	2.6597	0.4521	0.4543	1.4711	3.4365	2.6597	0.4521	0.4543
			\tilde{M}_X	1.3583	3.4095	2.4706	0.3661	0.2664	1.3584	3.4098	2.4709	0.3653	0.2680
m, n Up to 25	$c = 0$	\tilde{W}	—	—	—	—	—	—	—	—	—	—	
		\tilde{M}_X	1.4717	3.3789	2.6477	0.5384	0.3992	1.4727	3.3786	2.6482	0.5400	0.4018	
		$c = 5.0$	\tilde{W}	1.4711	3.4365	2.6597	0.4521	0.4543	1.4711	3.4365	2.6597	0.4522	0.4543
			\tilde{M}_X	1.3561	3.3987	2.4783	0.3476	0.2670	1.3559	3.3992	2.4774	0.3463	0.2698
m, n Up to 29	$c = 0$	\tilde{W}	—	—	—	—	—	—	—	—	—	—	
		\tilde{M}_X	—	—	—	—	—	1.4724	3.3783	2.6480	0.5401	0.4015	
		$c = 5.0$	\tilde{W}	—	—	—	—	—	—	—	—	—	—
			\tilde{M}_X	1.3565	3.4058	2.4706	0.3584	0.2509	1.3449	3.4017	2.4591	0.3467	0.2502
m, n Up to 33	$c = 0$	\tilde{W}	—	—	—	—	—	—	—	—	—	—	
		\tilde{M}_X	—	—	—	—	—	—	—	—	—	—	
		$c = 5.0$	\tilde{W}	—	—	—	—	—	—	—	—	—	—
			\tilde{M}_X	1.3554	3.4096	2.4689	0.3575	0.2583	1.3556	3.4104	2.4680	0.3536	0.2604
m, n Up to 35	$c = 0$	\tilde{W}	—	—	—	—	—	—	—	—	—	—	
		\tilde{M}_X	—	—	—	—	—	—	—	—	—	—	
		$c = 5.0$	\tilde{W}	—	—	—	—	—	—	—	—	—	—
			\tilde{M}_X	1.3550	3.3950	2.4682	0.3567	0.2569	1.3450	3.3954	2.4683	0.3533	0.2558

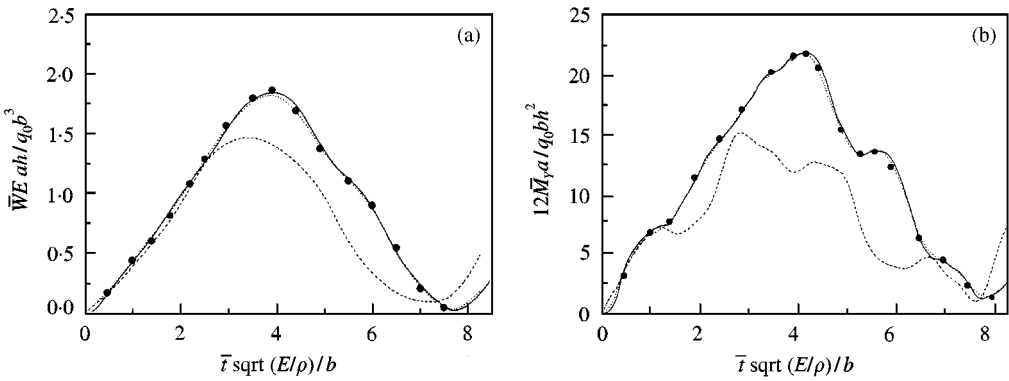


Figure 2. Comparisons of dynamic behaviors of rectangular plates under partially distributed step loads. (a) Central deflection versus time; (b) bending moment versus time: ●, Reddy [19]; ···, Reismann and Lee [18]; —, Present; --- CPT.

a Pasternak-type elastic foundation using both MSA and SVA of FSDPT, and are compared with their classical counterparts. It can be seen that dynamic responses obtained by MSA and SVA are identical, but CPT gives lower values of deflection and bending moment.

Figure 5 shows central deflection and bending moment as functions of time for an initially stressed thick square plate subjected to a suddenly applied central patch load and either resting on Pasternak-type or Winkler elastic foundations or without any elastic foundation. The stiffnesses are $(k_1, k_2) = (2.0, 1.0)$ and $(k_1, k_2) = (2.0, 0.5)$ for Pasternak-type elastic foundations and $(k_1, k_2) = (2.0, 0.0)$ and $(k_1, k_2) = (1.0, 0.0)$ for Winkler elastic foundations and $(k_1, k_2) = (0.0, 0.0)$ for the foundationless plate. It can be seen that the foundation stiffness has a significant effect on the dynamic response of the plate.

Figure 6 shows the effect of the flexural frequency (referred to as “low” in the figure) and the other two thickness-shear frequencies (referred to as “medium” and “high” in the figure) on the dynamic response of a thick square plate subjected to a suddenly applied central patch load combined with uniaxial compressive loads with or without thermal bending stress, when the plate is supported by a Pasternak-type elastic foundation. It can be seen that the thickness-shear frequencies have no effects on the dynamic response of the plate when there is no temperature loading. In contrast, they have small effects on the bending moment when thermal load is present.

Figure 7 shows the effect of the pulse shape and duration on the dynamic response of an initially stressed thick square plate under the loading condition of cases 1–5, i.e., sudden loads, step loads, triangular loads, sine loads and exponential loads in Table 1, when the plate is supported by a Pasternak-type elastic foundation. Here, $\bar{t}_0 \sqrt{E/\rho}/b$ ($= 5.0$ and 8.0) indicates pulse duration.

Figure 8 shows the effect of the loaded area parameter ($a_1/a = b_1/b = 0.5, 0.7,$ and 1.0) on the dynamic response of an initially stressed thick square plate subjected to a suddenly applied load and resting on a Pasternak-type elastic foundation. Note that $a_1/a = b_1/b = 1.0$ mean uniformly distributed load over the entire plate. As expected, these results show that the central deflections and bending moments are decreased by decreasing the loaded area parameter.

Figure 9 shows the effect of initial membrane stress on the dynamic response of a thick square plate subjected to a suddenly applied central patch load and resting on a Pasternak-type elastic foundation. Clearly, the in-plane loads have considerable effects on the dynamic behavior of the plate, but the biaxial load ratio has less effect.

TABLE 3
Comparison of the frequencies for initially stressed plates

In-plane loads	m	n	Reismann and Tendorf [2]			Present		
			$\Omega_{mn1}a\sqrt{\rho/E}$	$\Omega_{mn2}a\sqrt{\rho/E}$	$\Omega_{mn3}a\sqrt{\rho/E}$	$\Omega_{mn1}a\sqrt{\rho/E}$	$\Omega_{mn2}a\sqrt{\rho/E}$	$\Omega_{mn3}a\sqrt{\rho/E}$
$N_x = (N_x)_{cr}$	1	1	0.6175	20.0699	20.4474	0.6175	20.0653	20.4426
	1	3	1.5680	20.4448	21.7360	1.5667	20.4407	21.7317
	1	5	3.3748	21.1745	24.0084	3.3735	21.1700	24.0047
	5	1	6.0434	22.3268	27.0138	6.0180	22.2198	26.9321
	5	5	7.8790	23.3246	29.5552	7.8577	23.2223	29.4811
	5	10	12.5579	26.1989	36.1528	12.5447	26.1079	36.0922
	10	1	15.6193	28.2397	40.1144	15.5787	27.9002	39.8946
	10	20	29.3270	39.4308	61.7094	29.3152	39.1883	61.5622
$N_x = 0$	1	1	0.4366	20.0651	20.4428	0.4366	20.0653	20.4426
	1	3	1.5060	20.4401	21.7316	1.5060	20.4402	21.7316
	1	5	3.3464	21.1700	24.0044	3.3464	21.1700	24.0044
	5	1	5.6353	22.2199	26.9255	5.6353	22.2198	26.9254
	5	5	7.5705	23.2223	29.4745	7.5705	23.2223	29.4745
	5	10	12.3667	26.1078	36.0868	12.3667	26.1079	36.0868
	10	1	14.9967	27.9001	39.8761	14.9967	27.9002	39.8761
	10	20	29.0002	39.1884	61.5547	29.002	39.1883	61.5548
$N_x = -0.5(N_x)_{cr}$	1	1	0.3087	20.0627	20.4405	0.3087	20.0653	20.4425
	1	3	1.4740	20.4378	21.7294	1.4740	20.4378	21.7315
	1	5	3.3322	21.1678	24.0024	3.3329	21.1700	24.0043
	5	1	5.4198	22.1662	26.8811	5.4337	22.1662	26.9221
	5	5	7.4115	23.1709	29.4340	7.4227	23.1709	29.4712
	5	10	12.2700	26.0538	36.0538	12.2767	26.0621	36.0847
	10	1	14.6754	27.7288	39.7564	14.6969	27.7288	39.8671
	10	20	28.8353	39.0666	61.4773	28.8413	39.0666	61.5512

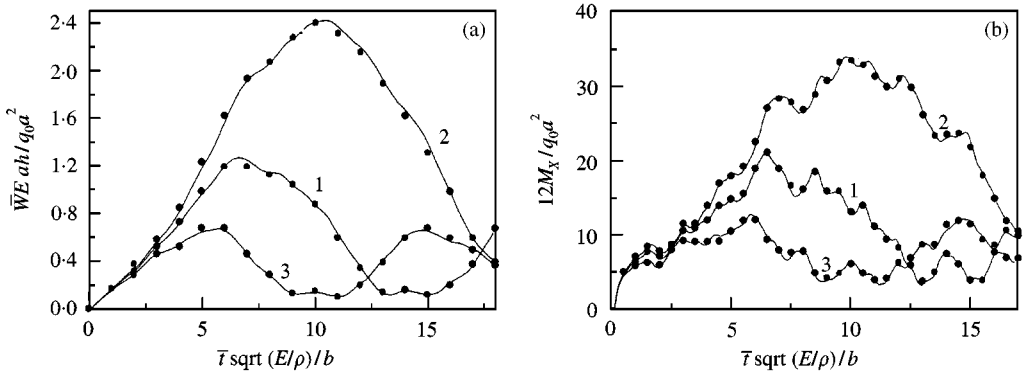


Figure 3. Comparisons of dynamic behaviors of initially stressed moderately thick plates under suddenly applied partially distributed loads. (a) Central deflection versus time; (b) bending moment versus time; ●, Reissmann and Tendorf [2]; —, Present; 1: $N_x = 0$; 2: $N_x = -0.5(N_x)_{cr}$; 3: $N_x = (N_x)_{cr}$.

TABLE 4

Comparison for thermal bending of a rectangular plate ($b/h = 1.5$)

h/a	Irschik and Pachinger [20]			Present	
	Analytical (CPT)	FEM (FSDPT)		FSDPT	
		All	0.1	0.3	0.1
$\frac{D\bar{W}}{\bar{M}^T a^2} \left(X = \frac{a}{2}, Y = \frac{b}{2} \right)$	0.101	0.101	0.101	0.1008	0.1008
$-\frac{\bar{M}_x}{\bar{M}^T(1-\nu)} \left(X = \frac{a}{2}, Y = \frac{b}{2} \right)$	0.238	0.239	0.239	0.2408	0.2408
$-\frac{\bar{M}_y}{\bar{M}^T(1-\nu)} \left(X = \frac{a}{2}, Y = \frac{b}{2} \right)$	0.762	0.764	0.763	0.7638	0.7638
$\frac{a\bar{Q}_x}{\bar{M}^T(1-\nu)} \left(X = 0, Y = \frac{b}{2} \right)$	0.758	0.000	0.000	0.000	0.000
$\frac{a\bar{Q}_y}{\bar{M}^T(1-\nu)} \left(X = \frac{a}{2}, Y = 0 \right)$	1.929	0.001	0.001	0.000	0.000

Figure 10 shows the effect of initial thermal bending stress ($C = 0.0, \pm 1.0$ and ± 5.0) on the dynamic response of an initially stressed thick square plate subjected to a suddenly applied central patch load and resting on a Pasternak-type elastic foundation. The temperature rise T_0 is taken as 30°C . It can be seen that, in the low-temperature case, these curves are very nearly coincident, whereas in the high-temperature case the thermal bending moment has a small effect on the curves.

Figures 11 and 12 show, respectively, plate width-to-thickness ratio b/h ($= 15.0, 10.0$ and 5.0) and plate aspect ratio β ($= 0.5, 1.0$ and 1.5) on the dynamic response of an initially stressed rectangular plate subjected to a suddenly applied central patch load and resting on a Pasternak-type elastic foundation. It can be seen that the transverse shear deformation has a significant effect on the dynamic behavior. Also, it can be seen that the central

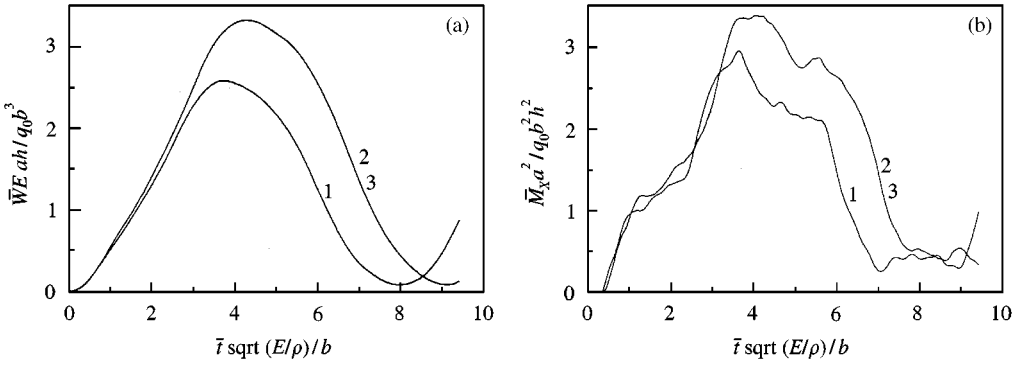


Figure 4. Comparisons of dynamic behaviors of a moderately thick plate obtained by various methods. (a) Central deflection versus time; (b) bending moment versus time ($\beta = 1.0, b/h = 10.0, T_0 = 0^\circ\text{C}, (k_1, k_2) = (2.0, 1.0), \chi = 0.0, N_x/(N_x)_{cr} = -0.25, a_1/a = b_1/b = 0.5$): 1: CPT; 2: MSA; 3: SVA.

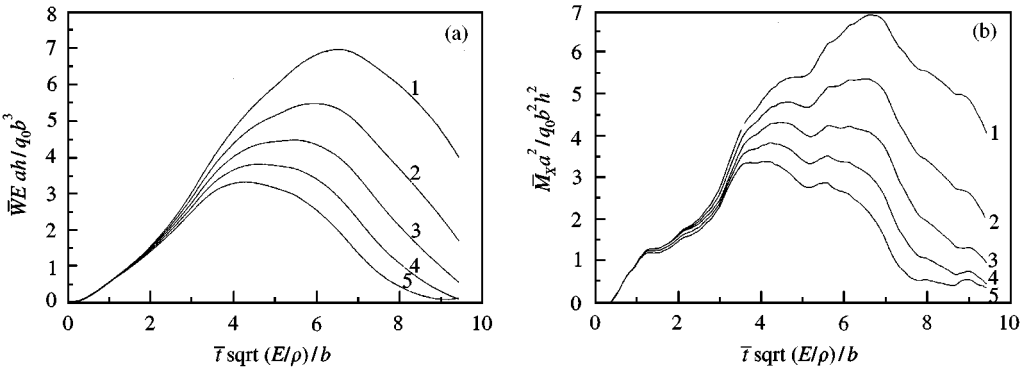


Figure 5. Effect of the foundation stiffness on dynamic behaviors of a moderately thick plate. (a) Central deflection versus time; (b) bending moment versus time ($\beta = 1.0, b/h = 10.0, T_0 = 0^\circ\text{C}, \chi = 0.0, N_x/(N_x)_{cr} = -0.25, a_1/a = b_1/b = 0.5$): 1: $(k_1, k_2) = (0.0, 0.0)$; 2: $(k_1, k_2) = (1.0, 0.0)$; 3: $(k_1, k_2) = (2.0, 0.0)$; 4: $(k_1, k_2) = (2.0, 0.5)$; 5: $(k_1, k_2) = (2.0, 1.0)$.

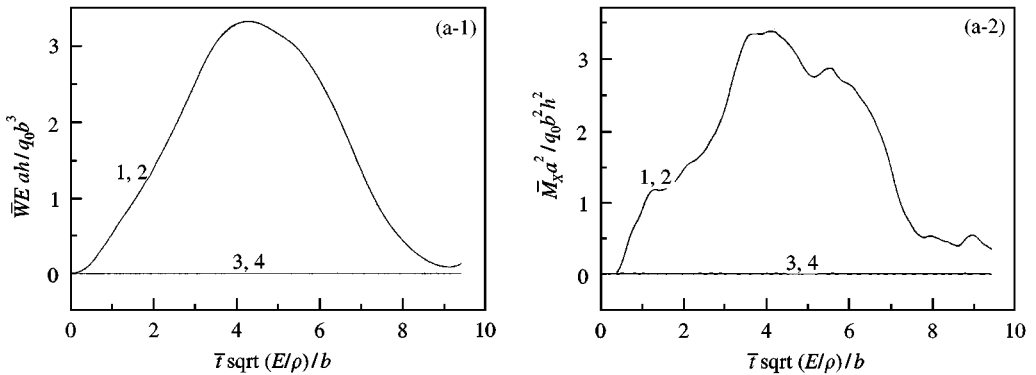


Figure 6. Effect of the modes on the dynamic behaviors of a moderately thick plate. (a-1,2) Central deflection and bending moment versus time without initial thermal bending; (b-1,2) central deflection and bending moment versus time with initial thermal bending ($\beta = 1.0, b/h = 10.0, \chi = 0.0, N_x/(N_x)_{cr} = -0.25, a_1/a = b_1/b = 0.5, (k_1, k_2) = (2.0, 1.0). T_0 = 0$ and 30°C respectively: 1: Low, medium, high; 2: Low; 3: Medium; 4: High.

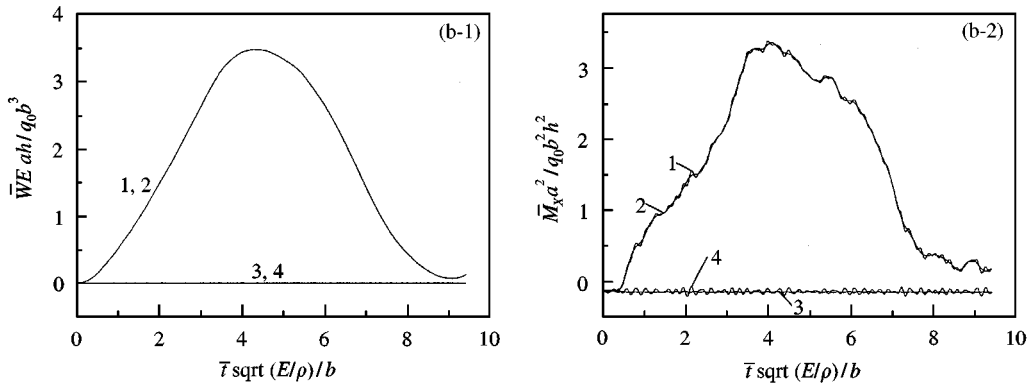


Figure 6. Continued.

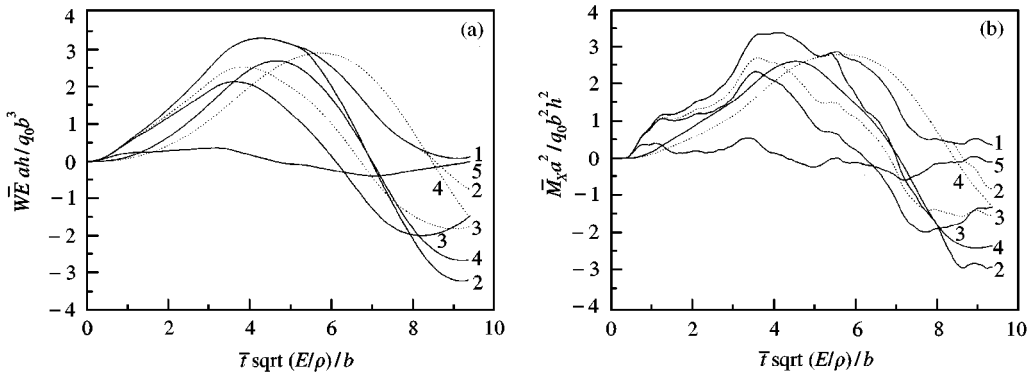


Figure 7. Effect of pulse shape and pulse duration on dynamic behaviors of a moderately thick plate. (a) Central deflection versus time; (b) bending moment versus time ($\beta = 1.0$, $b/h = 10.0$, $T_0 = 0^\circ\text{C}$, $(k_1, k_2) = (2.0, 1.0)$, $\chi = 0.0$, $N_x/(N_x)_{cr} = -0.25$, $a_1/a = b_1/b = 0.5$); 1: Load case 1; 2: Load case 2; 3: Load case 3; 4: Load case 4; 5: Load case 5; —, $\bar{t}_0\sqrt{E/\rho}/b = 5.0$; ---, $\bar{t}_0\sqrt{E/\rho}/b = 8.0$.

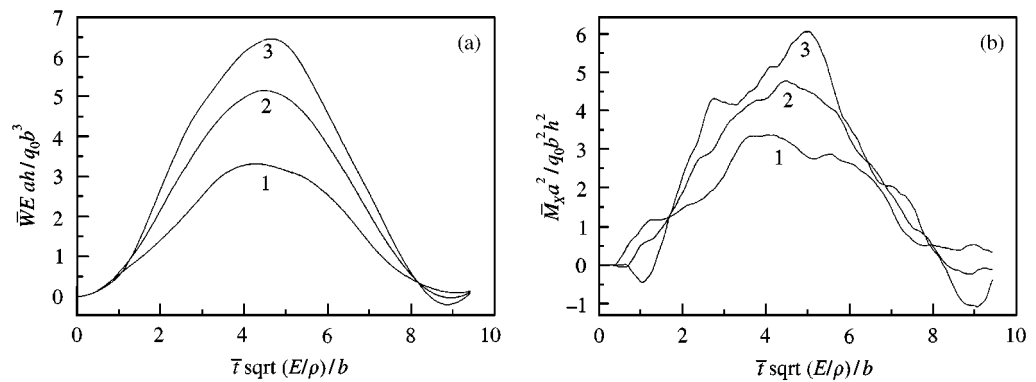


Figure 8. Effect of loaded area on dynamic behaviors of a moderately thick plate: (a) central deflection versus time; (b) bending moment versus time ($\beta = 1.0$, $b/h = 10.0$, $T_0 = 0^\circ\text{C}$, $(k_1, k_2) = (2.0, 1.0)$, $N_x/(N_x)_{cr} = -0.25$, $\chi = 0.0$): 1: $a_1/a = b_1/b = 0.5$; 2: $a_1/a = b_1/b = 0.7$; 3: $a_1/a = b_1/b = 1.0$.

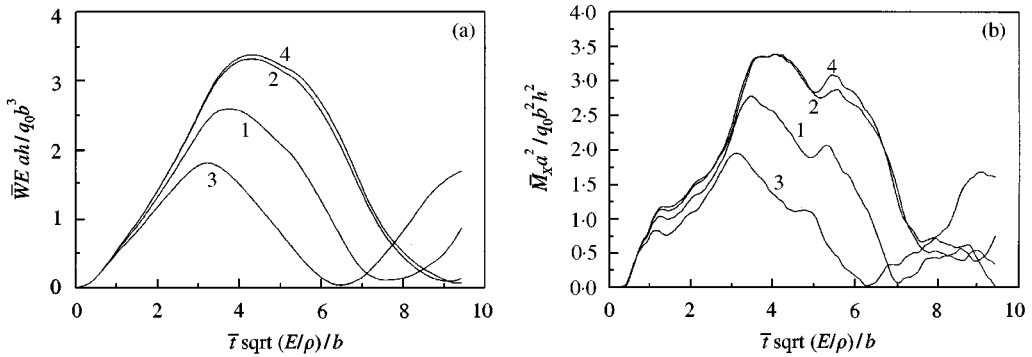


Figure 9. Effect of initial membrane stress on dynamic behaviors of a moderately thick plate: (a) central deflection versus time; (b) bending moment versus time ($\beta = 1.0$; $b/h = 10.0$, $T_0 = 0^\circ\text{C}$, $(k_1, k_2) = (2.0, 1.0)$, $a_1/a = b_1/b = 0.5$): 1: $\chi = 0.0$, $N_x/(N_x)_{cr} = 0.0$; 2: $\chi = 0.0$, $N_x/(N_x)_{cr} = -0.25$; 3: $\chi = 0.0$, $N_x/(N_x)_{cr} = 0.50$; 4: $\chi = 1.0$, $N_x/(N_x)_{cr} = -0.25$.

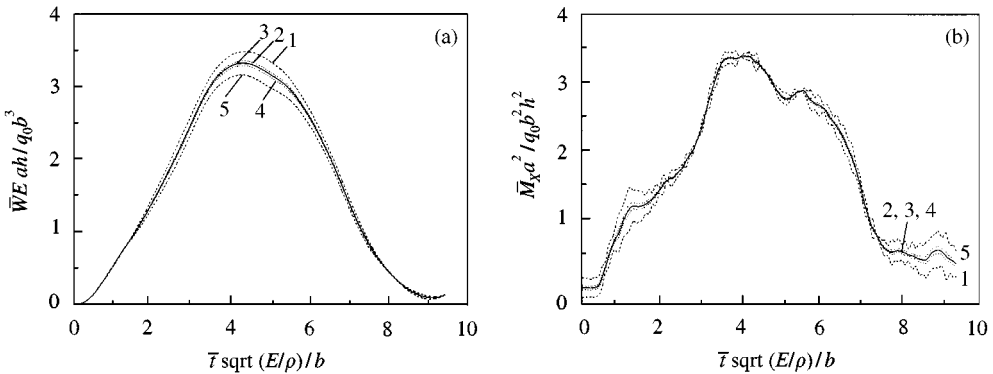


Figure 10. Effect of the initial thermal bending stress on dynamic behaviors of a moderately thick plate: (a) central deflection versus time; (b) bending moment versus time ($\beta = 1.0$, $b/h = 10.0$, $T_0 = 30^\circ\text{C}$, $(k_1, k_2) = (2.0, 1.0)$, $\chi = 0.0$, $N_x/(N_x)_{cr} = -0.25$, $a_1/a = b_1/b = 0.5$): 1,5: --- $c = \pm 5.0$; 2,4: $\cdots c = \pm 1.0$; 3: — $c = 0.0$.

deflections and bending moments are increased, but the frequency is decreased by increasing the plate aspect ratio.

In Figures 4–10 and 12, the plate width-to-thickness ratio $b/h = 10.0$; in Figures 4–7 and 9–12, the loaded area parameter $a_1/a = b_1/b = 0.5$; in Figures 4–8 and 10–12, the biaxial load ratio $\chi = 0.0$ and the initial compressive stress $N_x = -0.25(N_x)_{cr}$; and in Figures 4 and 6–12 the Pasternak-type elastic foundation stiffness is characterized by $(k_1, k_2) = (2.0, 1.0)$.

4. CONCLUSIONS

Dynamic behaviour of a simply supported Reissner–Mindlin plate under complex loading conditions and resting on a Pasternak-type elastic foundation has been studied by using the Modal Superposition Approach and the State Variable Approach respectively. A number of issues related to the static and dynamic behaviors of moderately thick plates without an elastic foundation have been examined.

A parametric study of moderately thick plates resting on Winkler or Pasternak-type elastic foundations has been carried out. The results show that the characteristics of

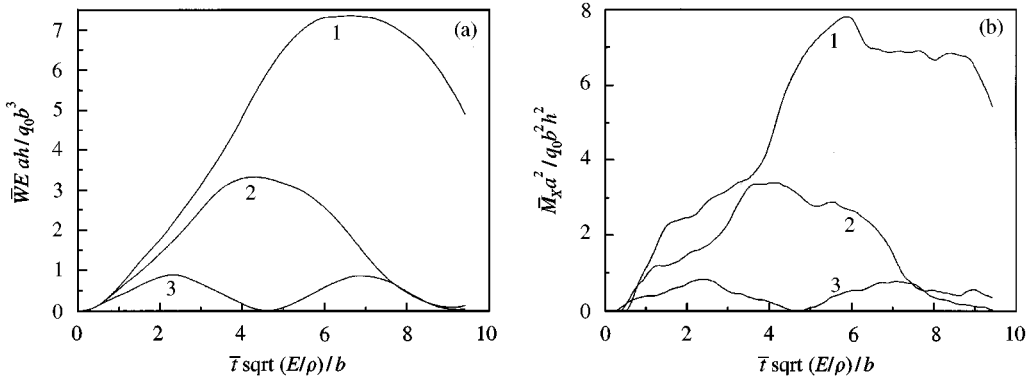


Figure 11. Effect of the plate width-to-thickness ratio on dynamic behaviors of a moderately thick plate: (a) central deflection versus time; (b) bending moment versus time ($\beta = 1.0$; $T_0 = 0^\circ\text{C}$, $(k_1, k_2) = (2.0, 1.0)$, $\chi = 0.0$, $N_x/(N_x)_{cr} = -0.25$, $a_1/a = b_1/b = 0.5$): 1: $b/h = 15.0$; 2: $b/h = 10.0$; 3: $b/h = 5.0$.

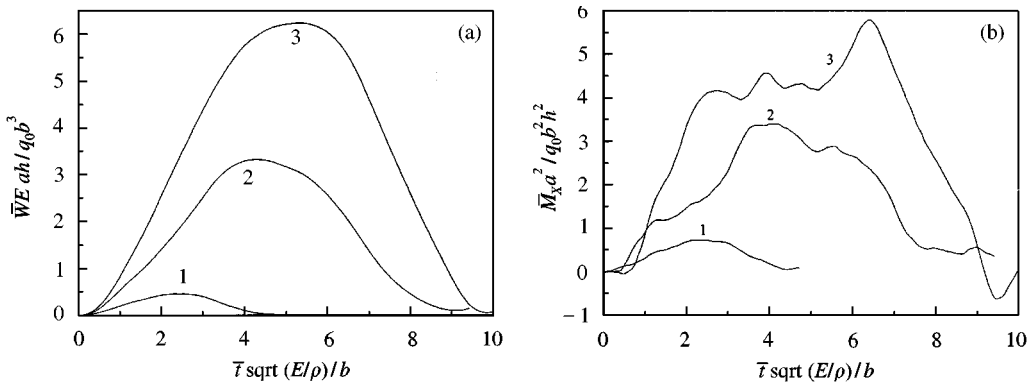


Figure 12. Effect of the plate aspect ratio on dynamic behaviors of a moderately thick plate. (a) Central deflection versus time; (b) bending moment versus time ($b/h = 10.0$, $T_0 = 0^\circ\text{C}$, $(k_1, k_2) = (2.0, 1.0)$, $N_x/(N_x)_{cr} = -0.25$, $a_1/a = b_1/b = 0.5$, $\chi = 0.0$): 1: $\beta = 0.5$; 2: $\beta = 1.0$; 3: $\beta = 1.5$.

dynamic behavior are significantly influenced by foundation stiffness, shape and duration of impulsive load, loaded area, transverse shear deformation, plate aspect ratio as well as initial membrane stress. In contrast, the initial thermal bending stress has rather less effect.

REFERENCES

1. A. L. DOBYNS 1981 *American Institute of Aeronautics and Astronautics Journal* **19**, 642–650. Analysis of simply-supported orthotropic plates subject to static and dynamic loads.
2. H. REISMANN and Z. A. TENDORF 1976 *Transactions of the ASME, Journal of Applied Mechanics* **43**, 304–308. Dynamics of initially stressed plates.
3. J. CHEN and D. J. DAWE 1996 *Composite Structures* **35**, 213–218. Linear transient analysis of rectangular laminated plates by a finite strip-mode superposition method.
4. C. T. SUN and J. M. WHITNEY 1976 *American Institute of Aeronautics and Astronautics Journal* **14**, 268–270. Dynamic response of laminated composite plates under initial stress.
5. A. A. KHDEIR and J. N. REDDY 1988 *Journal of Sound and Vibration* **126**, 437–445. Dynamic response of antisymmetric angle-ply laminated plates subjected to arbitrary loading.
6. Y. XIANG, C. M. WANG and S. KITIPORNCHAI 1994 *International Journal of Mechanics Sciences* **36**, 311–316. Exact vibration solution for initially stressed Mindlin plates on Pasternak foundations.

7. L. LIBRESCU and W. LIN 1997 *International Journal of Non-linear Mechanics* **32**, 211–225. Postbuckling and vibration of shear deformable flat and curved panels on a non-linear elastic foundation.
8. L. LIBRESCU, W. LIN, M. P. MEMETH and J. H. STARRES 1996 *American Institute of Aeronautics and Astronautics Journal* **34**, 166–177. Frequency–load interaction of geometrically imperfect curved panels subjected to heating.
9. H. S. SHEN 1995 *Engineering Structures* **17**, 523–529. Postbuckling analysis of moderately thick rectangular plates on two-parameter elastic foundations.
10. H. S. SHEN 1996 *Structural Engineering and Mechanics* **4**, 149–162. Thermomechanical postbuckling of imperfect moderate thick plates on two-parameter elastic foundations.
11. H. S. SHEN 1998 *ASCE Journal of Engineering Mechanics* **124**, 1080–1089. Large deflection of Reissner–Mindlin plates on elastic foundations.
12. K. J. BATHE and E. L. WILSON 1976 *Numerical Methods in Finite Element Analysis*. Englewood Cliffs, NJ: Prentice-Hall.
13. R. R. CRAIG 1979 *Structural Dynamic: An Introduction to Computer Methods*. New York: John Wiley.
14. S. S. RAO 1988 *The Finite Element Method in Engineering*. New York: Pergamon Press, second edition.
15. M. PETYT 1990 *Introduction to Finite Element Vibration Analysis*. Cambridge: Cambridge University Press.
16. A. A. KHDEIR and J. N. REDDY 1989 *International Journal of Mechanical Sciences* **31**, 499–510. On the forced motions of antisymmetric cross-ply laminated plates.
17. A. A. KHDEIR and J. N. REDDY 1989 *Composites Science and Technology* **34**, 205–224. Exact solutions for the transient response of symmetric cross-ply laminates using a higher-order plate theory.
18. H. REISMANN and Y. LEE 1969 in *Developments in Theoretical and Applied Mechanics* Vol. **4**, (D. FRDERICK, editor), 3–18. Forced motions of rectangular plates. New York: Pergamon Press.
19. J. N. REDDY 1982 *International Journal for Numerical Methods in Engineering* **19**, 237–255. Dynamic (transient) analysis of layered anisotropic composite-material plates.
20. H. IRSCHIK and F. PACHINGER 1995 *Journal of Thermal Stresses* **18**, 59–68. On thermal bending of moderately thick polyganal plates with simply supported edges.
21. R. D. MINDLIN and L. E. GOODMAN 1950 *Journal of Applied Mechanics* **17**, 377–380. Beam vibrations with time-dependent boundary conditions.
22. Y. Y. YU 1960 *Journal of Applied Mechanics* **27**, 535–540. Forced flexural vibrations of sandwich plates in plane strain.

APPENDIX A

In equations (15) and (16), ignoring external forces, the solution of free vibration of the plate is assumed as

$$\begin{aligned}
 W_{mn}(x, y, t) &= W_{mn}(x, y)T_{mn}(t), \\
 \Psi_{xmn}(x, y, t) &= \Psi_{xmn}(x, y)T_{mn}(t), \\
 \Psi_{ymn}(x, y, t) &= \Psi_{ymn}(x, y)T_{mn}(t),
 \end{aligned} \tag{A1}$$

where $T_{mn}(t) = e^{i\omega_{mnt}}$ ($i = \sqrt{-1}$), and $W_{mn}(x, y)$, $\Psi_{xmn}(x, y)$, $\Psi_{ymn}(x, y)$ are the shape functions for (m, n) modal and can be assumed to have the form

$$\begin{aligned}
 W_{mn}(x, y) &= W_{mn} \sin mx \sin ny, \\
 \Psi_{xmn}(x, y) &= \Psi_{xmn} \cos mx \sin ny, \\
 \Psi_{ymn}(x, y) &= \Psi_{ymn} \sin mx \cos ny \quad (m, n = 1, 2, 3, \dots).
 \end{aligned} \tag{A2}$$

Substituting equation (A1) into equations (15)–(17) in which the external impulsive and thermal loads are ignored, yields the following eigenvalue problem:

$$\begin{bmatrix} a_{11} - \omega_{mn}^2 & a_{12} & a_{13} \\ a_{21} & a_{22} - \omega_{mn}^2 & a_{23} \\ a_{31} & a_{32} & a_{33} - \omega_{mn}^2 \end{bmatrix} \begin{Bmatrix} W_{mn} \\ \Psi_{xmn} \\ \Psi_{ymn} \end{Bmatrix} = 0, \tag{A3}$$

where

$$a_{11} = \frac{(1 + K_2\gamma + \lambda_x\gamma)m^2 + (1 + K_2\gamma + \lambda_y\gamma\beta^2)n^2\beta^2 + K_1\gamma}{\theta^2\gamma},$$

$$a_{12} = \frac{m}{\theta^2\gamma}, \quad a_{13} = \frac{n\beta}{\theta^2\gamma}, \quad a_{21} = \frac{m}{\gamma}, \quad a_{22} = m^2 + v_1n^2\beta^2 + \frac{1}{\gamma}, \quad a_{23} = v_2mn\beta,$$

$$a_{31} = \frac{n\beta}{\gamma}, \quad a_{32} = a_{23}, \quad a_{33} = v_1m^2 + n^2\beta^2 + \frac{1}{\gamma}. \tag{A4}$$

The frequency and corresponding vibration modal shape functions can be obtained by calculating eigenvalues and eigenvectors of the coefficient matrix of equation (A3). For each modal shape function there exist three sequent frequencies, namely, low, medium and high ones in which the low one represents the flexural frequency and the other two represent thickness-shear frequencies.

Following Mindlin and Goodman [21] and Yu [22] the orthogonality condition of the principal modes can be established as

$$\int_0^\pi \int_0^\pi [\theta^2 W_{mn}^{(p)}(x, y)W_{kl}^{(q)}(x, y) + \Psi_{xmn}^{(p)}(x, y)\Psi_{xkl}^{(q)}(x, y) + \Psi_{ymn}^{(p)}(x, y)\Psi_{ykl}^{(q)}(x, y)] dx dy$$

$$\begin{cases} = 0 & \text{when } m \neq k \text{ or } n \neq l \text{ or } p \neq q, \\ \neq 0 & \text{when } m = k \text{ and } n = l \text{ and } p = q, \end{cases} \tag{A5}$$

where $m, n, l = 1, 2, 3, \dots, p, q = 1, 2, 3$.

Because of equations (A3) and (A4), it is mentioned that equation (A5) has the same form as in references [21, 22], but it contains terms in K_1 and K_2 .